Supporting Information

A Ratiometric Fluorescent Sensor Based on Carbon Dots Encapsulated in ZIF-8 for Visual Discrimination and Detection of Tetracycline and Chlortetracycline

Jin Wang, Baojie Liu, Jixing Liang, Hongguo Hao, Yaoyao Wang, Yunwu Li,* and Suna Wang*

Shandong Provincial Key Laboratory of Chemical Energy Storage and Novel Cell Technology, School of Chemistry and Chemical Engineering, Liaocheng University, Liaocheng, 252059, P. R. China

Table of content.

Fig. S28. (a) and (b) Variation trend of the inhibition efficiency with the concentration of TC and CTC under the influence of the IFE.

Fig. S29. (a) and (b) The luminescence lifetime decay curves of **CDs@ZIF-8** and **CDs@ZIF-8** with TC and CTC.

Fig. S30. (a-e) XPS spectra of **CDs@ZIF-8** before and after immersion in TC and high resolution regions of Zn2p, C1s, N1s and O1s, respectively.

Fig. S31. (a-e) XPS spectra of **CDs@ZIF-8** before and after immersion in CTC and high resolution regions of Zn2p, C1s, N1s and O1s, respectively.

Table S1. Application of CDs@ZIF-8 fluorescent probes.

CDs@MOFs composites	Analyte	Precursors of CDs	Response model	λ_{em} (λ_{ex})	LOD	Linear range	*Refs.*
yCDs/ZIF-8	Fe^{3+}	yCDs: Succinic anhydride, *o*-PD; BCDs: CA, Tris	Ratiometric fluorescence	465 nm (BCDs), 540 nm (YCDs) (λ_{ex} =380 nm)	0.3690 μM	10-80 μM,	41
QDs/CDs@ZIF-8	Cu^{2+}	CA, DETA	Ratiometric fluorescence	430 nm (CDs), 620 nm (QDs) (λ_{ex} =370 nm)	1.53 nM	5-100 nM	42
N-CD/R-CD @ZIF-8	Pb^{2+}	N-CDs：CA, UREA; R-CDs: Spinach	Ratiometric fluorescence	440 nm (N-CDs), 680 nm (R-CDs) (λ_{ex} =340 nm)	4.78 nM	0.05-50 μM	40
CDs@ZIF-8	Cu^{2+}	CA, EDA	turn off	430 nm (CDs) (λ_{ex} =345 nm)	0.26 mM	0-550 mM	43
CDs@ZIF-8	Fe^{3+}	CA, UREA	turn off	450 nm (λ_{ex} =365 nm)	5.2 μM	0.1-1 mM	44
CD/CdTe QD@ZIF-8	Ag^{+}	CA, DETA	Ratiometric fluorescence	430 nm (CDs)，650 nm (QDs) (λ_{ex} =365 nm)	1.49 nM	0.1-20 μM	45
CDs@ZIF-8	S^{2-}	processed gasoline	turn on	435 nm (CDs) (λ_{ex} =365 nm)	330 nM	1-400 μM	46
BYCDs@ZIF-8	Glutathione	Y-CDs: *o*-PD: B-CDs: CA, UREA	Ratiometric fluorescence	440 nm (BCDs), 565nm (YCDs) (λ_{ex} =365nm)	0.90 nM	3-25 nM	47
CDs&ZIF-8@MIPs	Malachite Green	sweet osmanthus leaf	turn off	440 nm	2.93 nM	20-180 nM	48
NCDs@ZIF-L	PA	CA, EDA	turn off	453 nm (NCDs)	0.139 μM	0.099-2.75 μM	49
CDs@ZIF-8	DA	GSH, CA	turn off	432 nm (CDs) (λ_{ex} =347 nm)	16.64 nM	0.1-200 μM	50
CDs/AuNCs @ZIF-8	ATP		Ratiometric fluorescence	469 nm (CDs), 660 nm (AuCNs) (λ_{ex} =360 nm)	0.061 μM	0.2-100 μM	32
CDs@ZIF-8	Sudan dyes	CA, UREA	turn off	518 nm (CDs) (λ_{ex} =410 nm)	76.56 nM	0.25-70 μM	51
CDs@ZIF-8	TC/CTC	*p*-PD, UREA	Ratiometric fluorescence	332 nm (ZIF-8), 492 nm (CDs) (λ_{ex} =275 nm)	7.13 nM/7.25nM	0-6μM	this work

Table S2. Fluorescent sensing of TCs by CDs@ZIF-8.

CDs@MOFs composites	Analyte	Precursors of CDs	Response model	$\lambda_{em}(\lambda_{ex})$	LOD（μM）	Linear range（μM）	*Refs.*
CDs/QDs@ZIF-8	TC	L-Cys, CA	Ratiometric fluorescence	427 nm (CDs), 520nm (TC), 618nm (QD) (λ_{ex} =350 nm)	0.0142	5×10^{-4}-0.050	52
gCDs@ZIF-8	TC	Glu, ammonia, glacial acetic acid	turn off	480 nm (CDs) (λ_{ex} =360 nm)	0.157	0–0.050	53
CDs/ST@ZIF-8	TC	PEI,CA	Ratiometric fluorescence	440 nm, 570 nm (λ_{ex} =360 nm)	0.046	0.200–10.0	54
ZIF-8/CDs	TC	CA, EDA	Ratiometric fluorescence	466 nm (CDs), 516 nm (TC)	0.01613	0.03–60	55
CuNCs@ZIF-8	TC	-	Ratiometric fluorescence	520 nm (TC), 606 nm (CuCNs)	0.034	0.1–50	56
ZIF-8&N-CDs@MIP	TC	CA, UREA	turn off	440 nm (CDs) (λ_{ex} =360 nm)	0.1013	0.225–9.00	57
CD@ZIF	TC	L-Cys, CA	turn off	427 nm (CDs), 520 nm (TC), 720 nm (SOS) (λ_{ex} =360 nm)	0.027	0.1–40	58
Znq2@ZIF-8	TC	-	turn off	495 nm	0.13	0–50	59
Fe_3O_4QDs@ZIF-8	TC	$FeCl_3$, $C_6H_5Na_3O_7$	turn off	A 652 nm	0.0338	0.225–45.0	60
ZIF-8@SDS	TC	-	turn on	521 nm (TC)	9×10^{-3}	0.01 ~ 60	61
ZIF-8	TC	-	Ratiometric fluorescence	445 nm (ZIF-8), 505 nm (TC) (λ_{ex} =375nm)	0.0147	225–2.25×10^{4}	62
CDs@ZIF-8	TC/CTC	*p*-PD, UREA	Ratiometric fluorescence	332 nm (ZIF-8), 492 nm (CDs) (λ_{ex}=275nm)	7.13×10^{-3}/7.25×10^{-3}	0–6	This work

Table S3. Parameters of the IFE of TC on the **CDs@ZIF-8** composite material.

TC(μM)	A_{ex}	A_{em}	CF	F_{obs}	F_{corr}	E_{obs}	E_{corr}
0	0.429	0.373	2.31	6470	14950	0	0
1	0.498	0.413	2.57	3824	9833	0.409	0.342
2	0.524	0.432	2.69	3208	8618	0.504	0.424
3	0.593	0.452	2.84	2475	7021	0.617	0.530
5	0.630	0.468	2.92	2300	6718	0.645	0.551

(CF=F_{corr}/F_{obs}, CF refers to the IFE correction parameter measured in TC solutions of varying concentrations; E_{obs}=1-$F_{obs}/F_{obs,0}$; E_{corr}=1-$F_{corr\ s}/F_{corr,0}$)

Table S4. Parameters of the IFE of CTC on the **CDs@ZIF-8** composite material.

CTC(μM)	A_{ex}	A_{em}	CF	F_{obs}	F_{corr}	E_{obs}	E_{corr}
0	0.438	0.367	2.31	6653	15410	0	0
1	0.542	0.395	2.62	3834	10080	0.424	0.345
2	0.671	0.466	2.85	2260	6433	0.660	0.583
3	0.796	0.552	2.88	1361	3924	0.795	0.745
5	0.923	0.587	2.85	1017	2895	0.847	0.812

(CF=F_{corr}/F_{obs}, CF refers to the IFE correction parameter measured in CTC solutions of varying concentrations; $E_{obs}=1-F_{obs}/F_{obs,0}$; $E_{corr}=1-F_{corr\ s}/F_{corr,0}$)

Table S5. Effects of CDs@ZIF-8 on the detection of TC in tap water.

Sample	Analyte	Add/μM	Found[a] (mean ± SD)/μM	Recovery (%)	RSD[b] (n = 3, %)
TC	tap water	1	0.96±0.02	96.33	2.16
		3	2.90±0.15	96.89	5.29
		5	4.89±0.10	97.80	1.97

[a] Concentrations are reported as mean ± SD (n=3). [b] RSD = (SD/mean)×100%

Table S6. Effects of CDs@ZIF-8 on the detection of CTC in tap water.

Sample	Analyte	Add/μM	Found[a] (mean ± SD)/μM	Recovery (%)	RSD[b] (n = 3, %)
CTC	tap water	1	0.98±0.05	97.67	4.73
		3	2.97±0.05	98.89	1.66
		5	5.01±0.24	100.13	4.74

[a] Concentrations are reported as mean ± SD (n=3). [b] RSD = (SD/mean)×100%

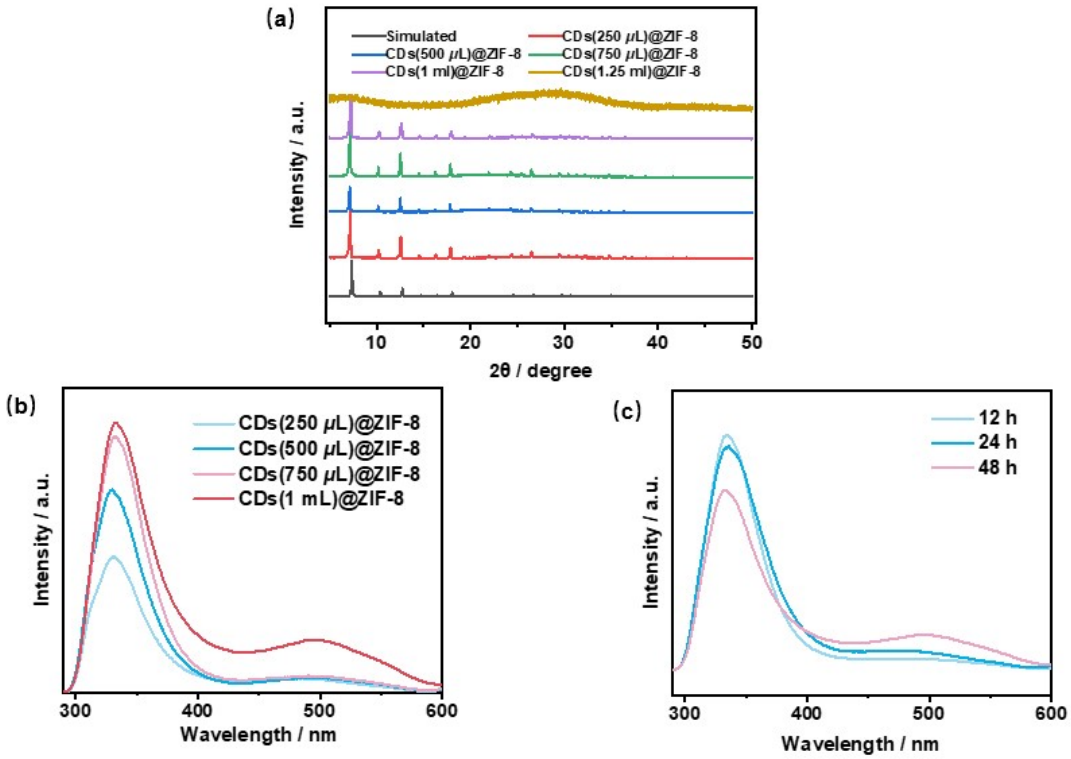

Fig. S1. (a) PXRD patterns and (b) fluorescence spectra of as-synthesized composites with different CDs dispersion loading volumes. (c) Fluorescence spectra of **CDs@ZIF-8** at different standing times (12 h, 24 h and 48 h).

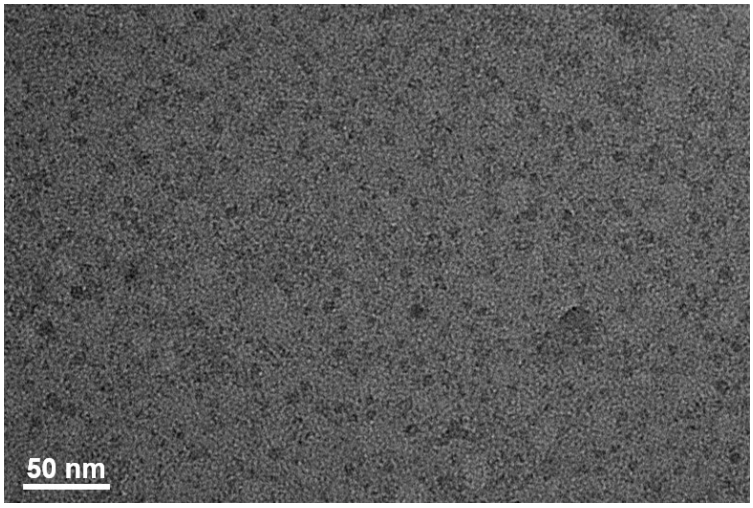

Fig. S2. HR-TEM of CDs.

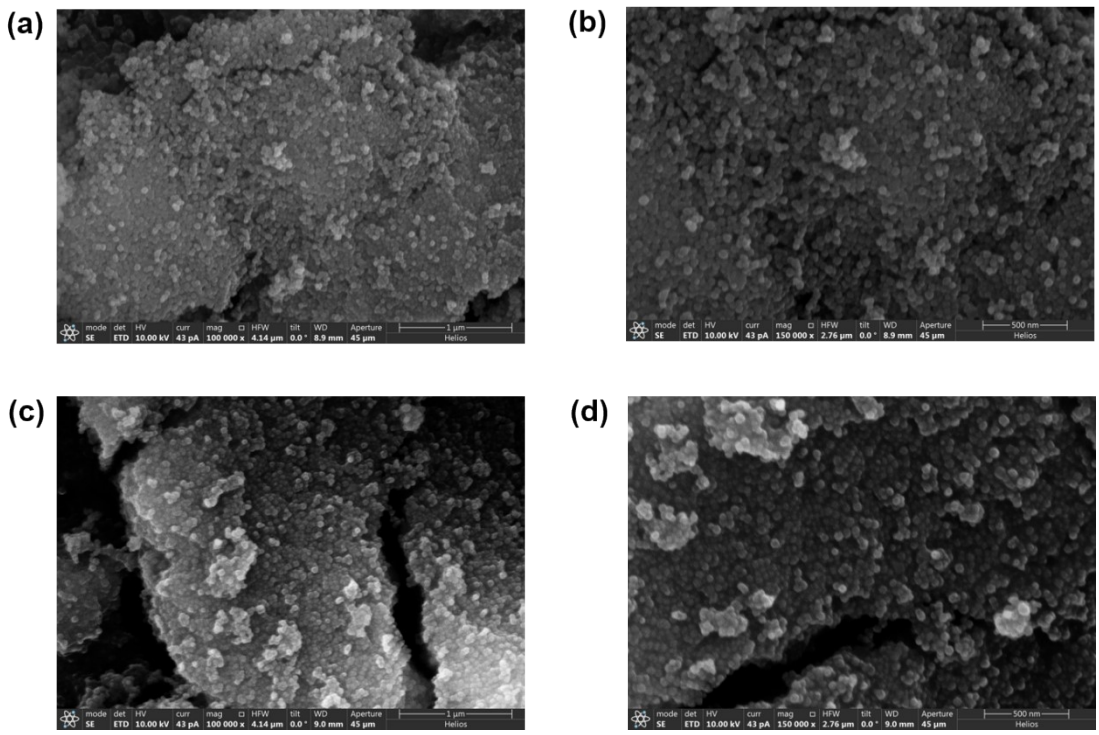

Fig. S3. (a-b) SEM of **ZIF-8**, (c-d) SEM of **CDs@ZIF-8**.

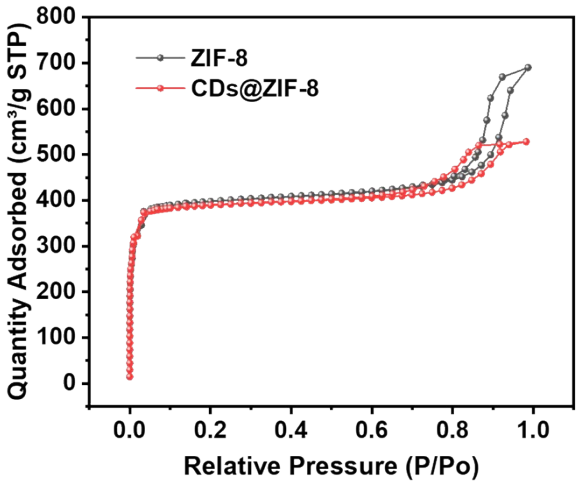

Fig. S4. N_2 absorption-desorption isotherms of pure **ZIF-8** (black) and **CDs@ZIF-8** (red) collected at 77 K.

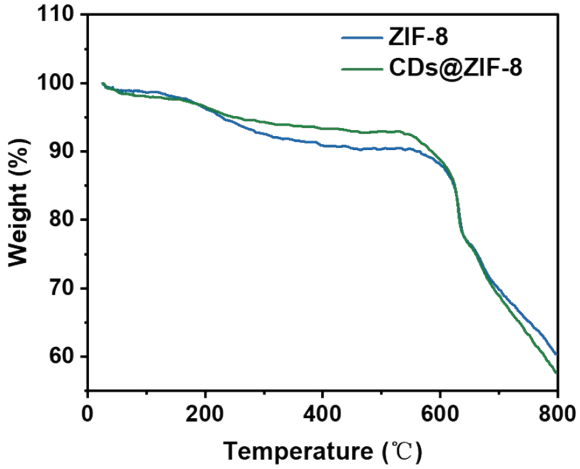

Fig. S5. TG of **ZIF-8** and **CDs@ZIF-8**, respectively.

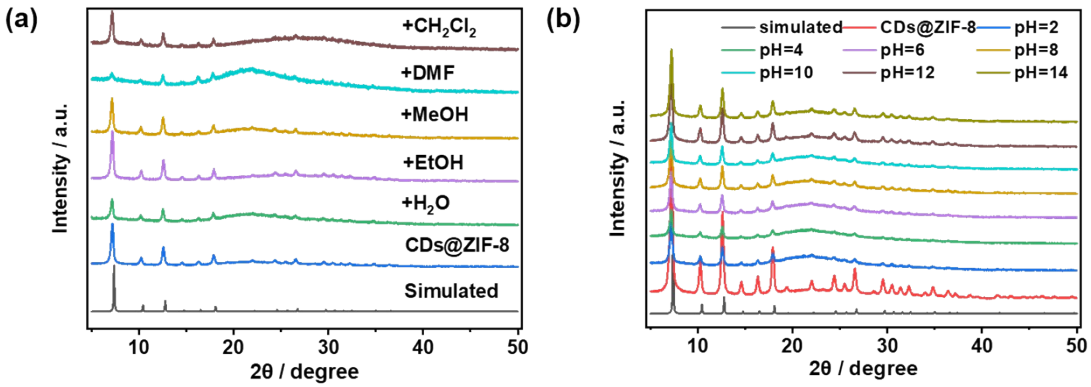

Fig. S6. (a) and (b) PXRD spectra of **CDs@ZIF-8** composites under different solvents and solution pH values.

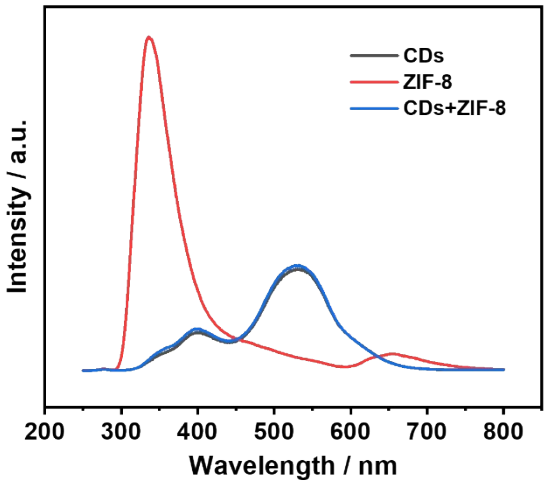

Fig. S7. Luminescence spectra of **CDs, ZIF-8** and simple mixture of **ZIF-8** and **CDs.**

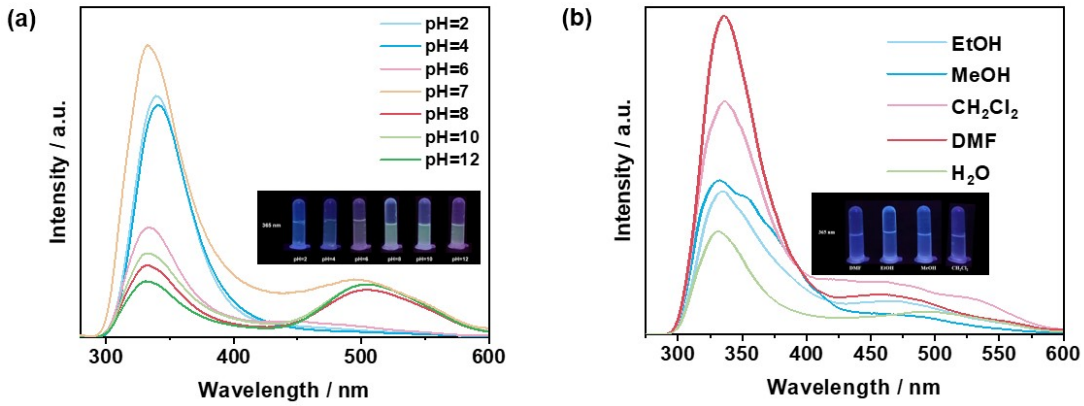

Fig. S8. (a) and (b) Fluorescence spectra of **CDs@ZIF-8** in solution with different pH values and common solvents.

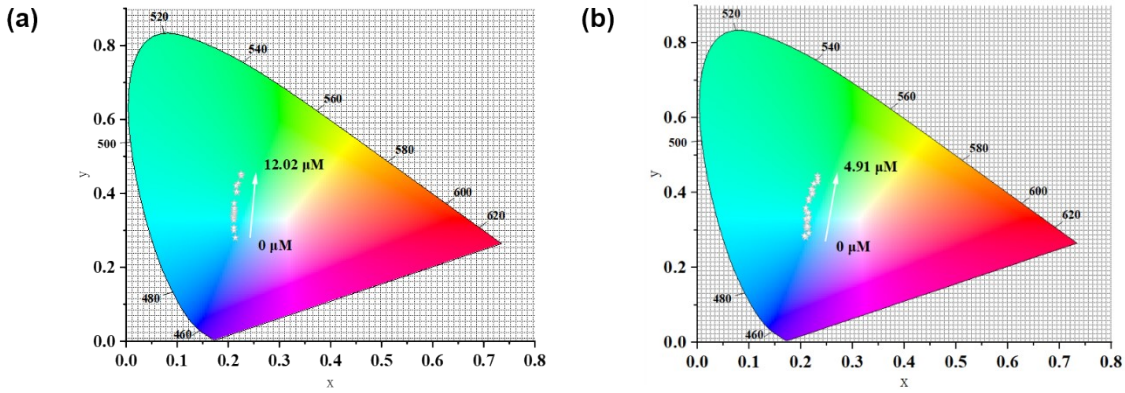

Fig. S9. (a) and (b) CIE coordinates for TC and CTC fluorescence titration.

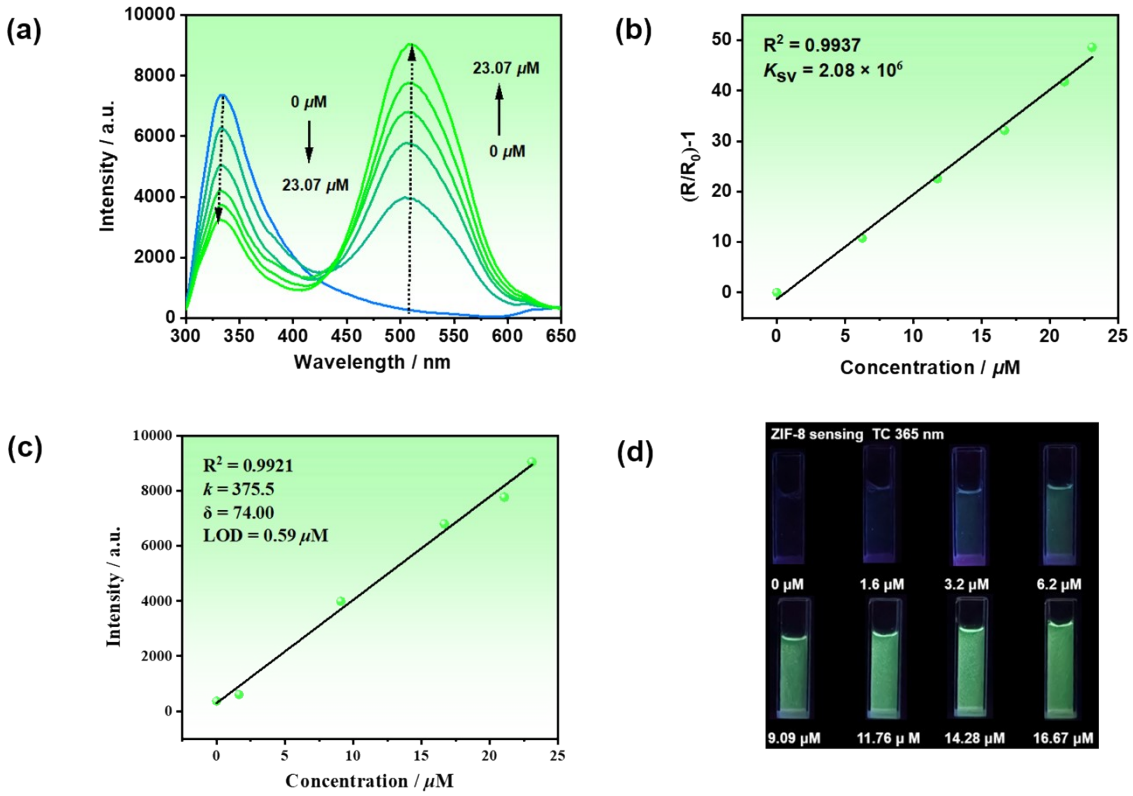

Fig. S10. (a) Luminescence titration spectra of **ZIF-8** toward TC. (b) The linear relationship of the luminescence intensity dependence upon **TC** concentration for **ZIF-8** towards TC. (c) The detection limit calculation of **ZIF-8 (10^{-3} M)** towards **TC**. (d) The photos of **ZIF-8** suspensions with different **TC** concentrations under UV light of 365 nm.

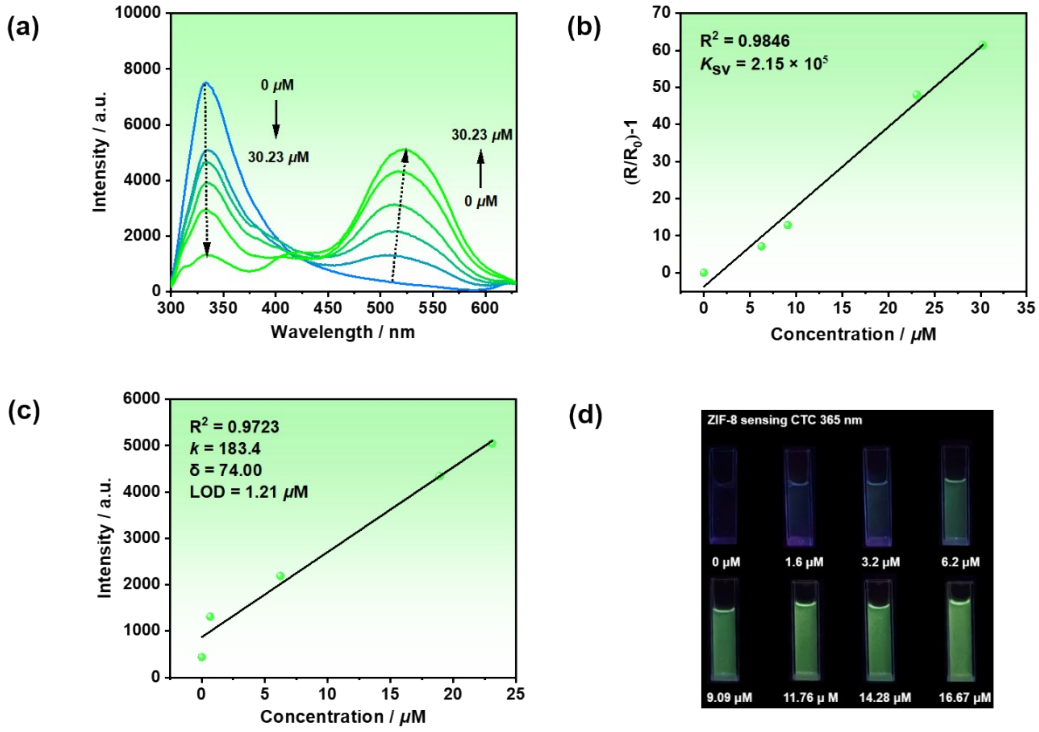

Fig. S11. (a) Luminescence titration spectra of **ZIF-8** toward CTC. (b) The linear relationship of the luminescence intensity dependence upon CTC concentration for **ZIF-8** towards TC. (c) The detection limit calculation of **ZIF-8** (10^{-3} M) towards TC. (d) The photos of **ZIF-8** suspensions with different CTC concentrations under UV light of 365 nm.

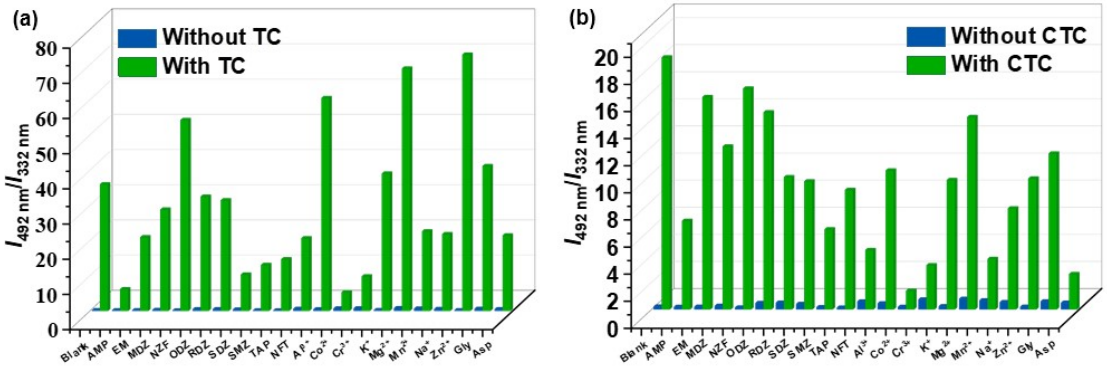

Fig. S12. (a) and (b) Luminescence intensities of **CDs@ZIF-8** in different coexisted substances with and without TC and CTC.

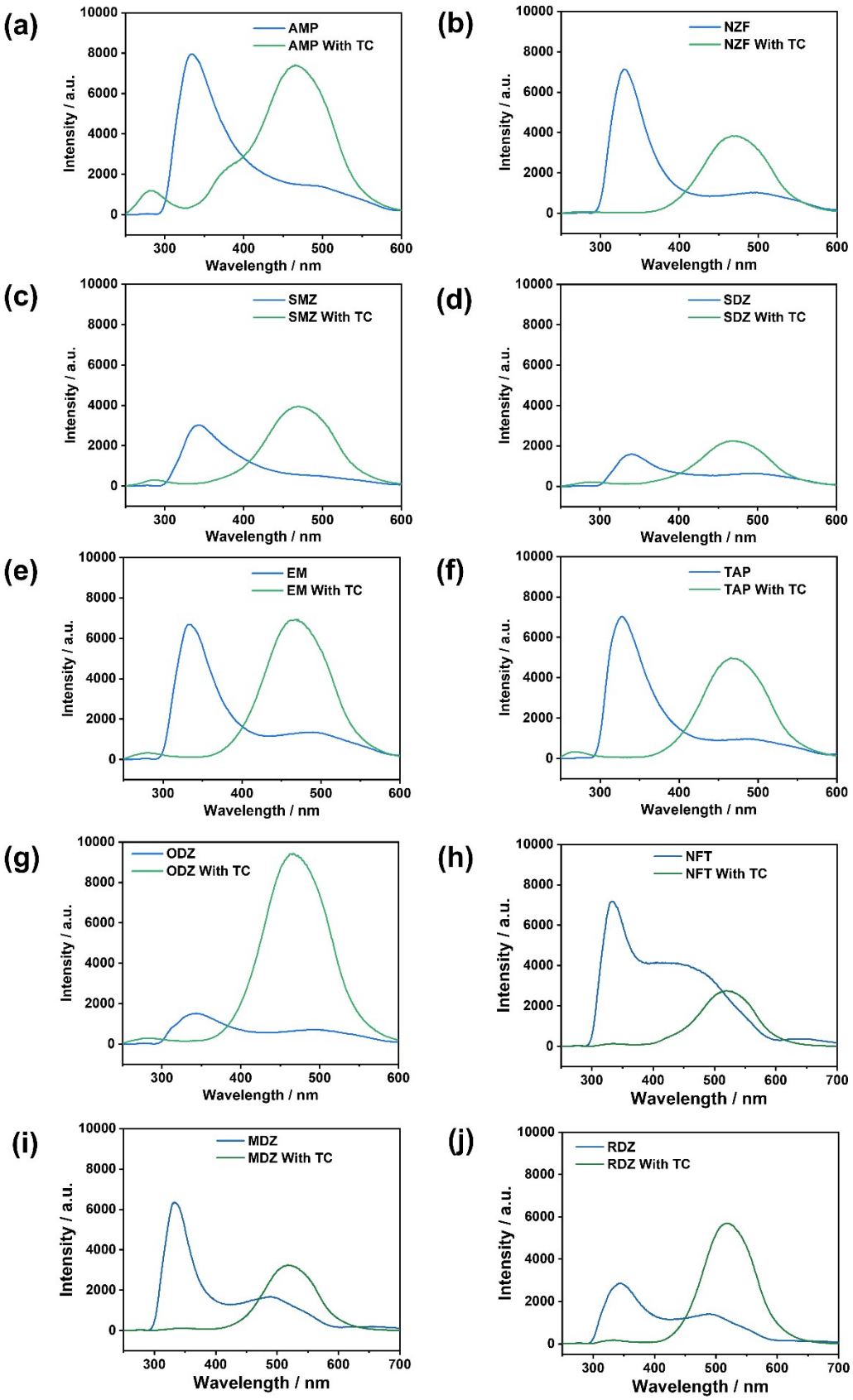

Fig. S13. (a-j) The luminescence emission of **CDs@ZIF-8** toward other antibiotic solutions with and without TC.

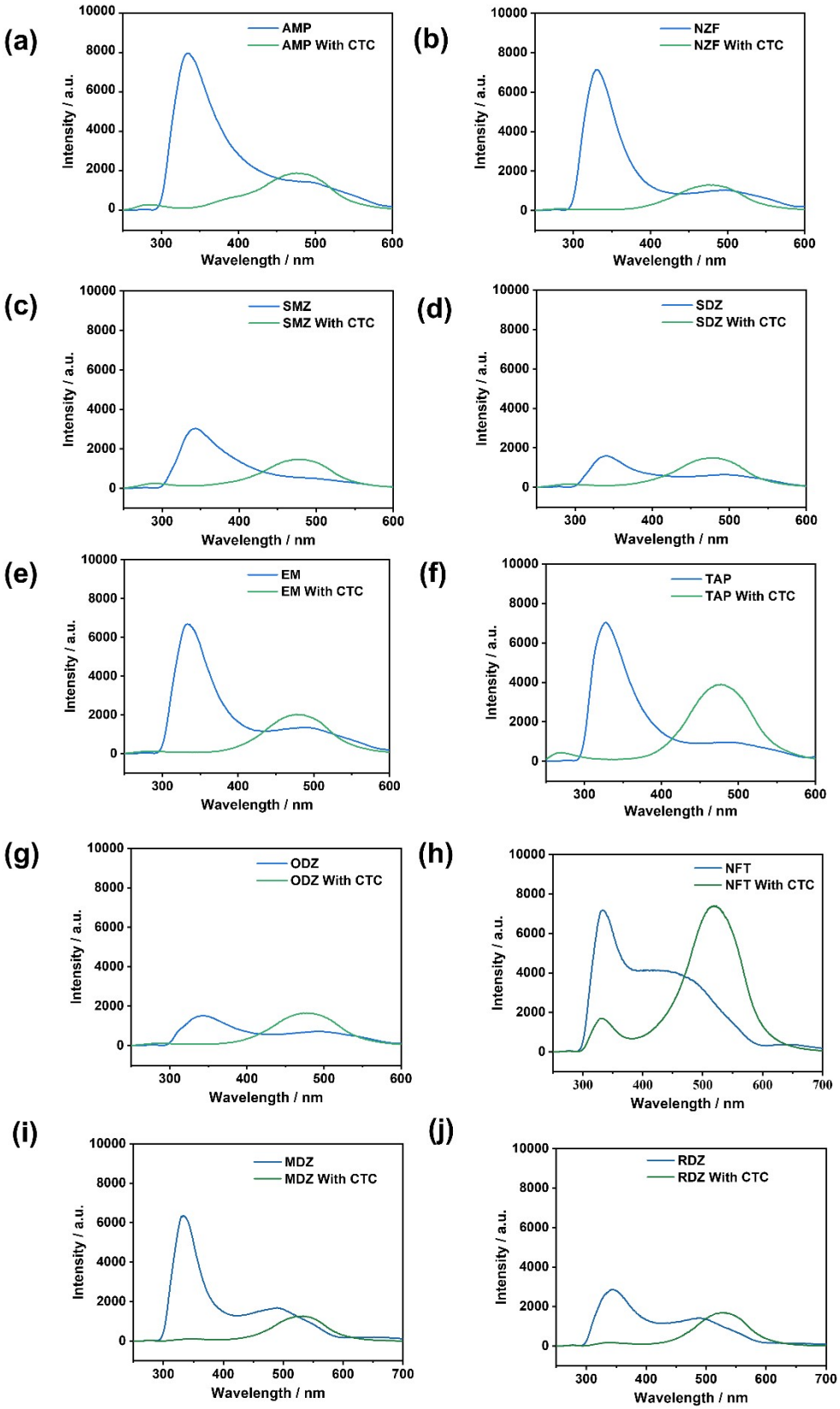

Fig. S14. (a-j) The luminescence emission of **CDs@ZIF-8** toward other antibiotic solutions with and without CTC.

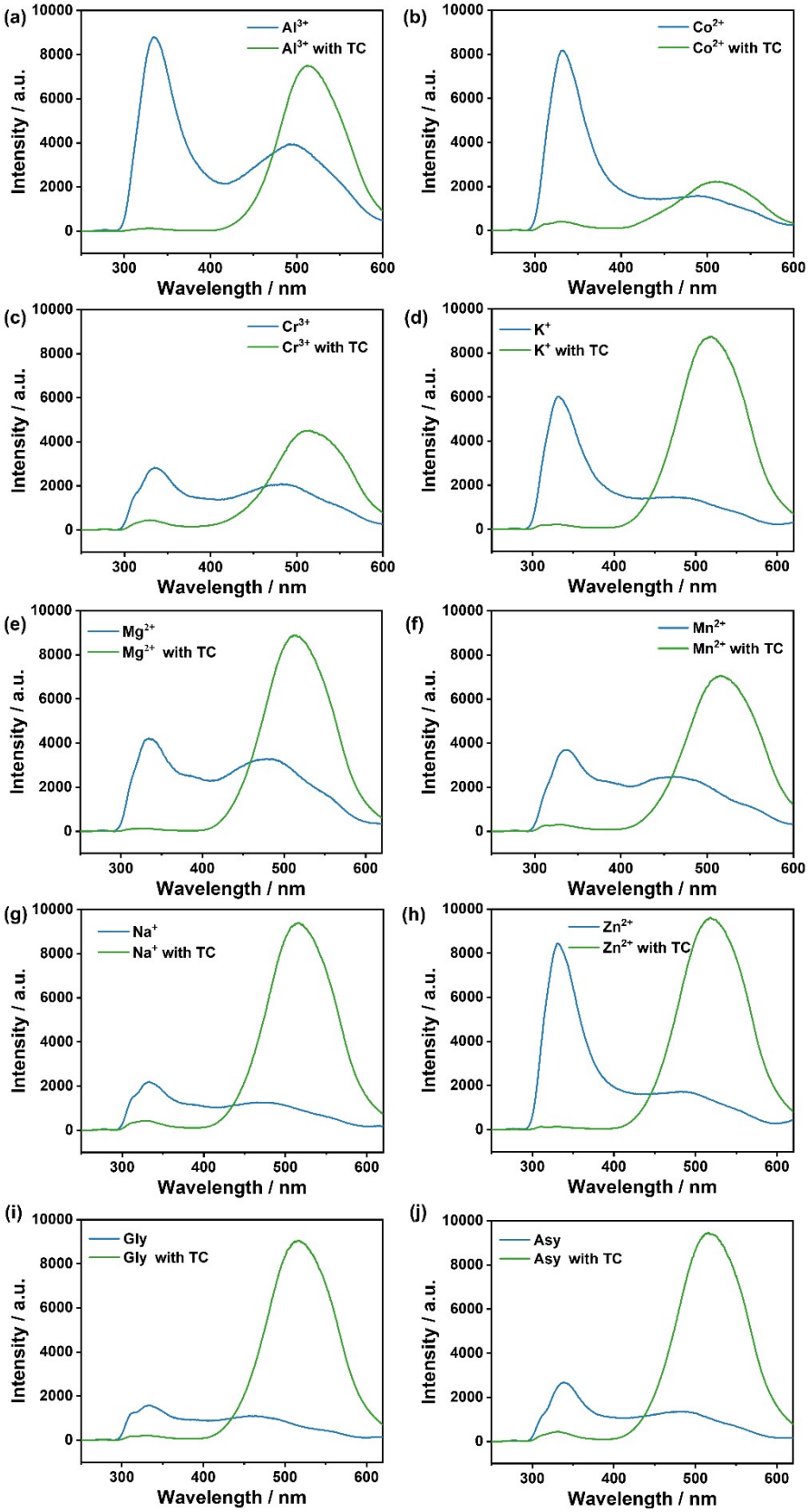

Fig. S15. (a-j) The luminescence emission of **CDs@ZIF-8** toward various inorganic ion and amino acid solutions with and without TC.

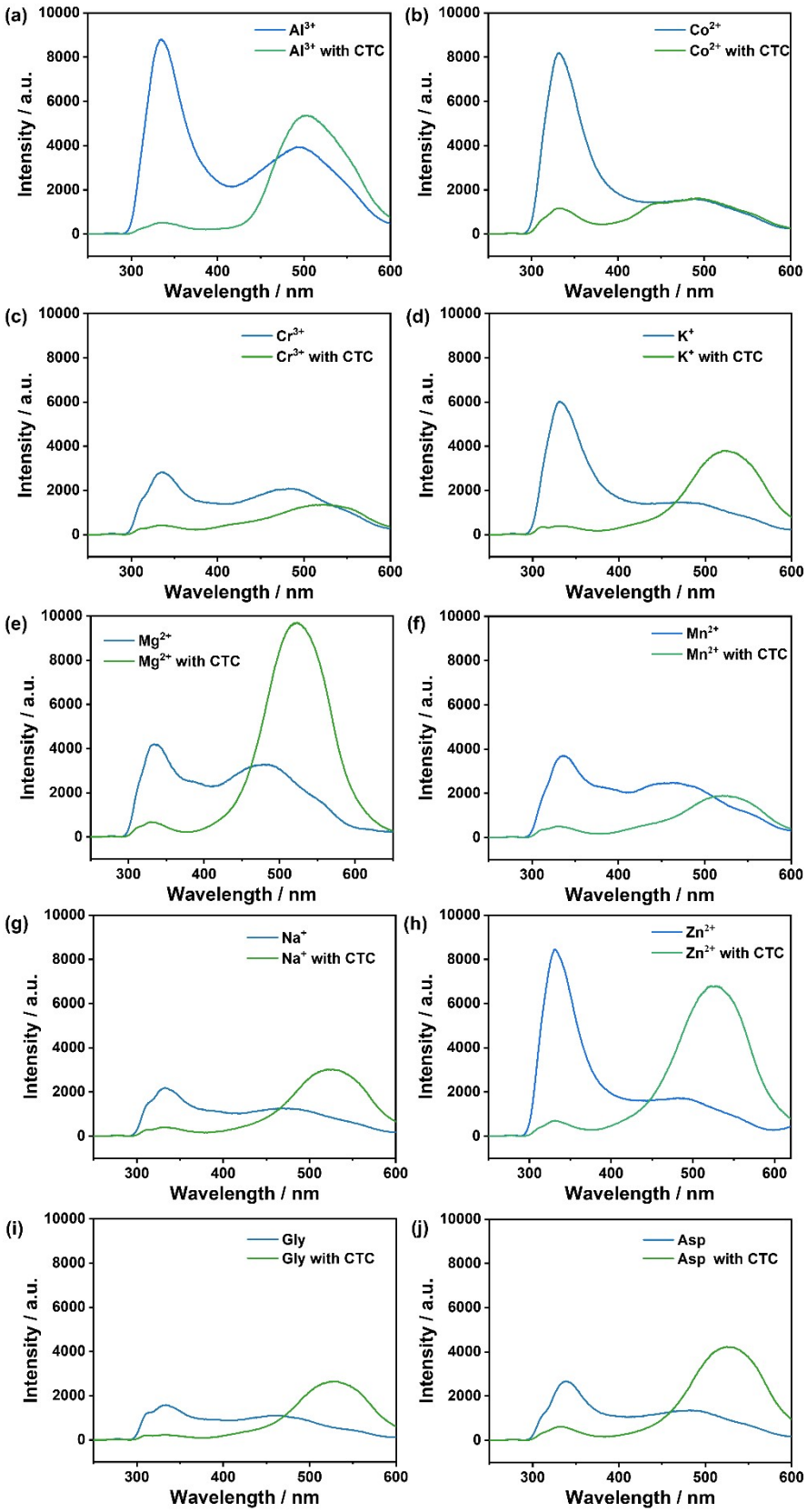

Fig. S16. (a-j) The luminescence emission of **CDs@ZIF-8** toward various inorganic ion and amino acid solutions with and without CTC.

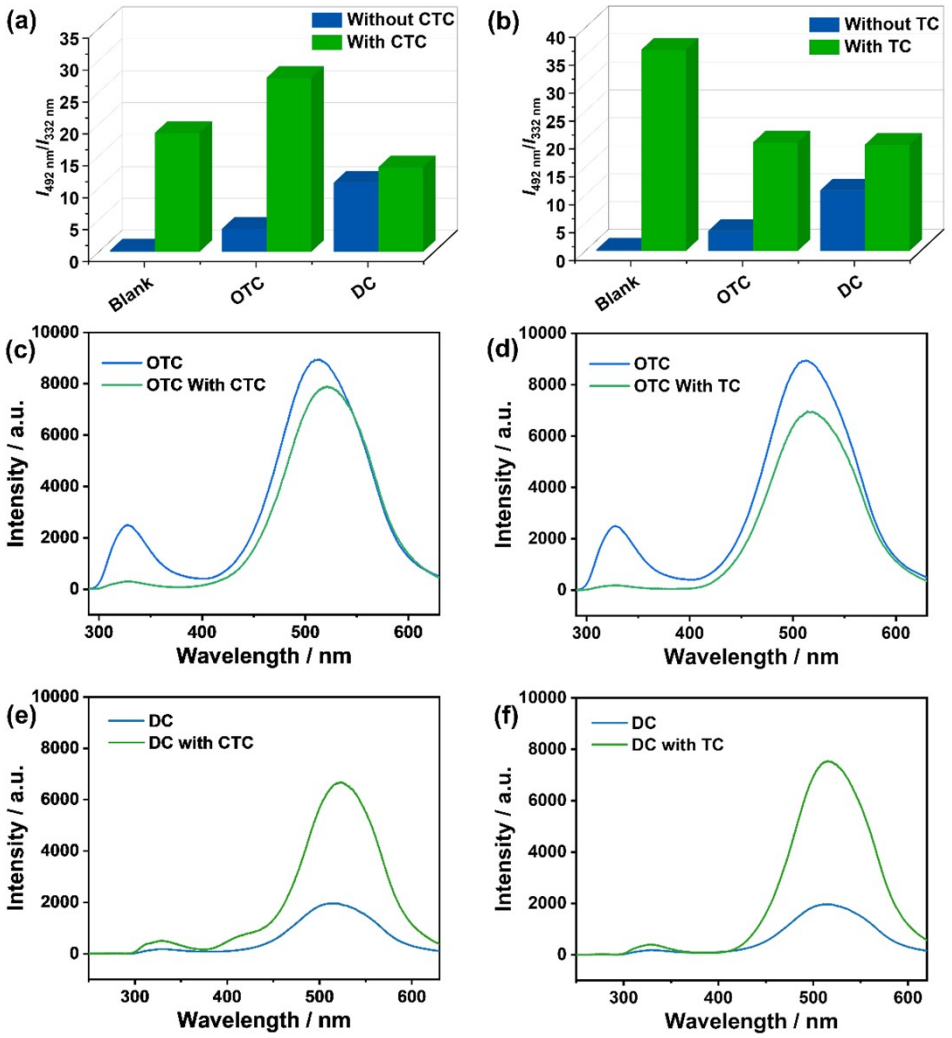

Fig. S17. (a) and (b) Luminescence intensities of **CDs@ZIF-8** toward OTC/DC solutions with and without CTC and TC. (c-f) The luminescence spectra of **CDs@ZIF-8** toward OTC and DC with and without CTC and TC.

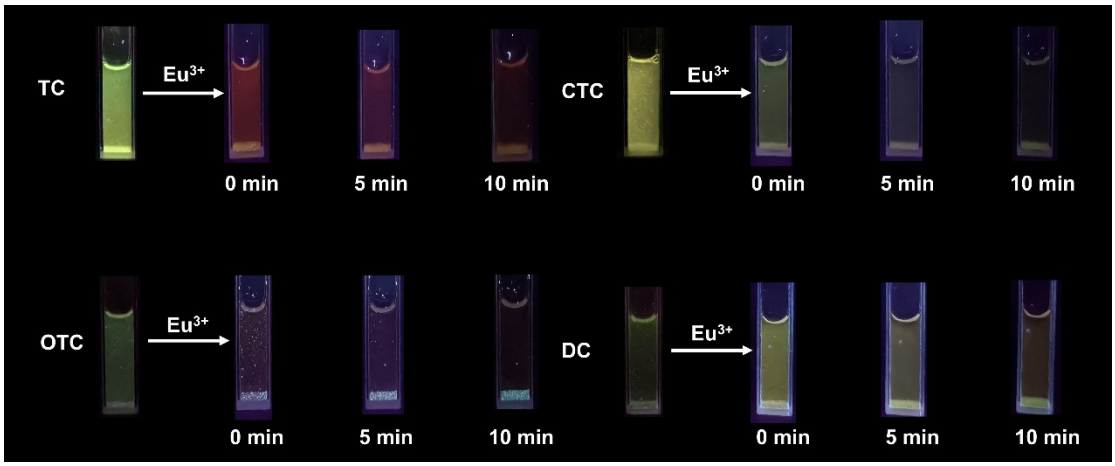

Fig. S18. Fluorescence photographs of **CDs@ZIF-8** in four TC antibiotics under 365 nm UV light after the addition of Eu^{3+}.

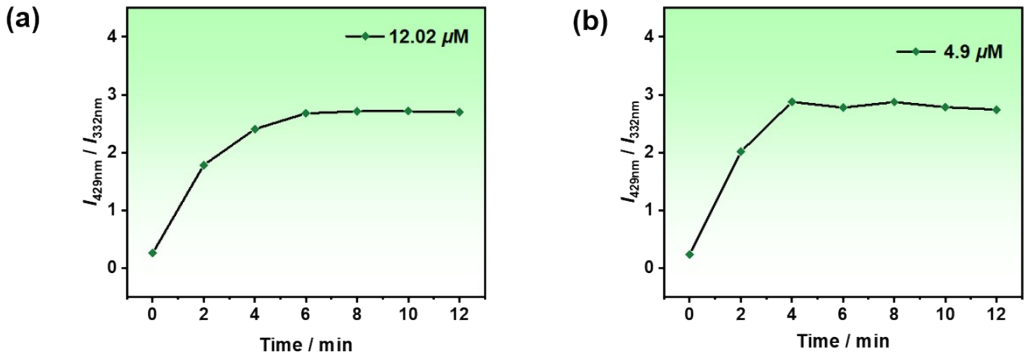

Fig. S19. (a) and (b) Response time results of **CDs@ZIF-8** toward TC and CTC under 275 nm excitation.

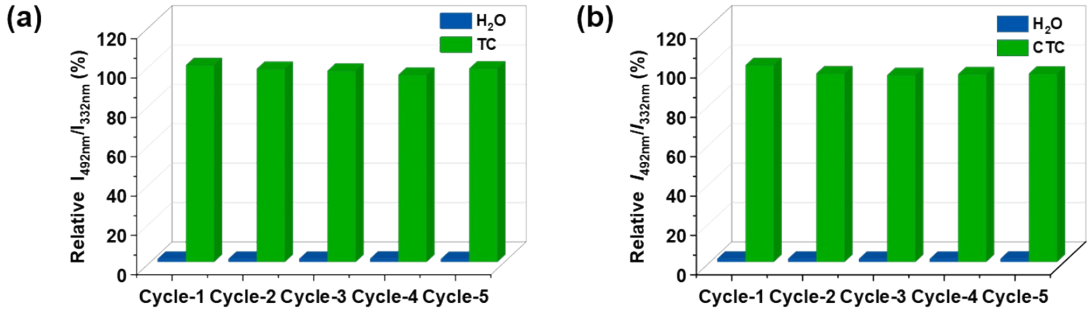

Fig. S20. (a) TC and (b) Five-cycle repeatability of the sensing performance of **CDs@ZIF-8** toward TC and CTC under 275 nm excitation.

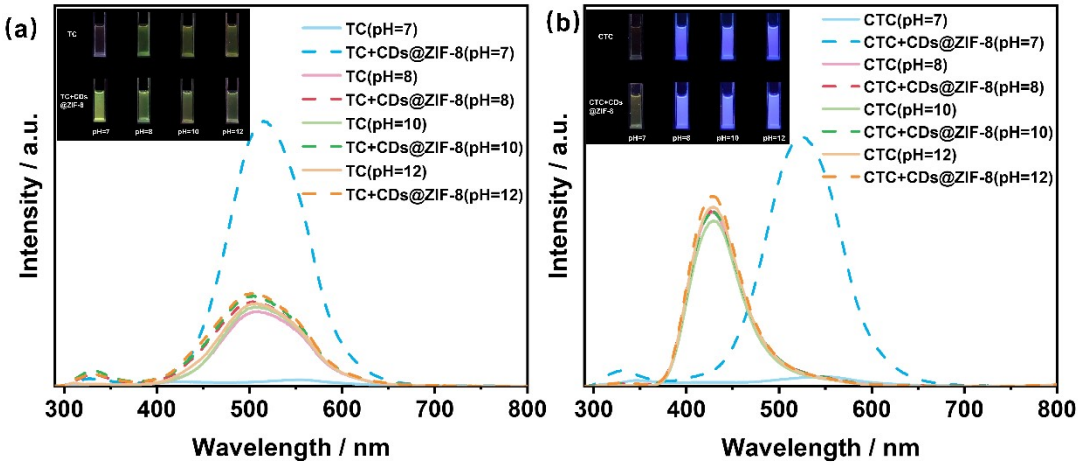

Fig. S21. (a) and (b) Fluorescence spectra and fluorescence photographs under UV light of TC and CTC under neutral and alkaline conditions.

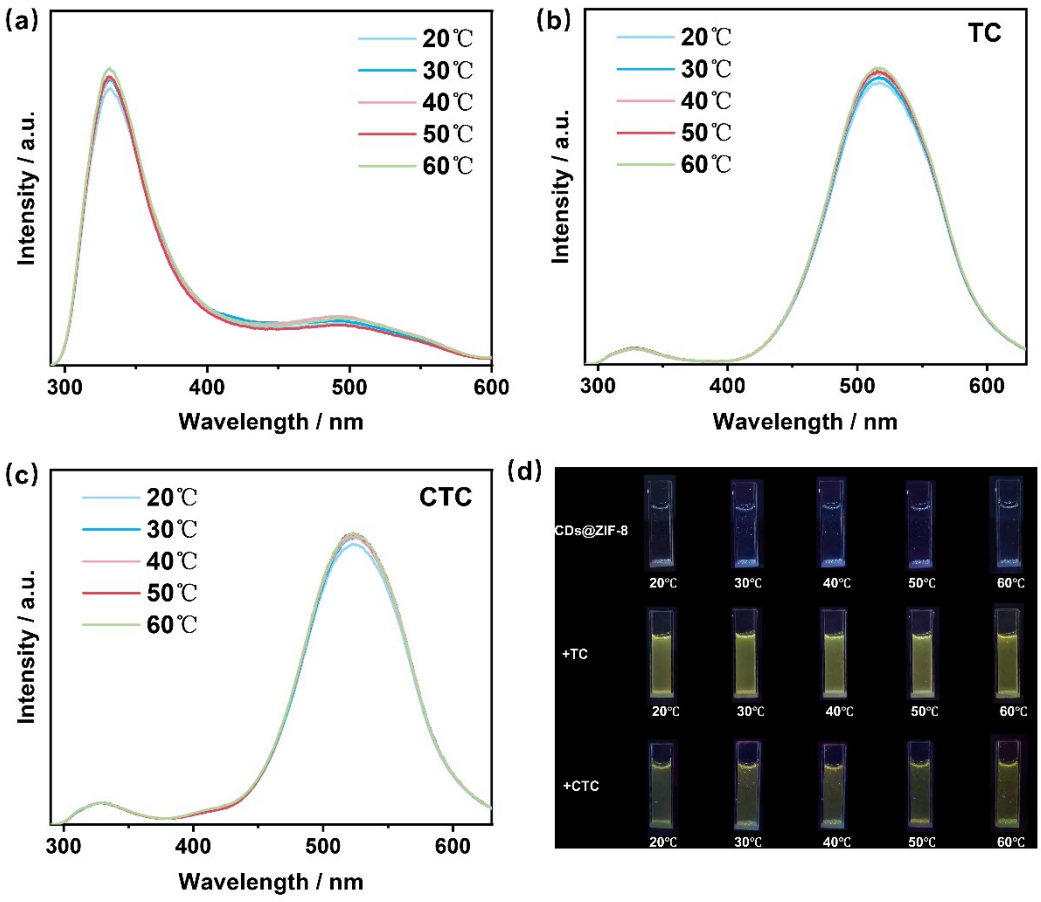

Fig. S22. Fluorescence spectra and fluorescence photographs under different temperature conditions: (a) **CDs@ZIF-8**; (b) **CDs@ZIF-8**+TC; (c) **CDs@ZIF-8**+CTC; (d) Fluorescence photographs under UV light.

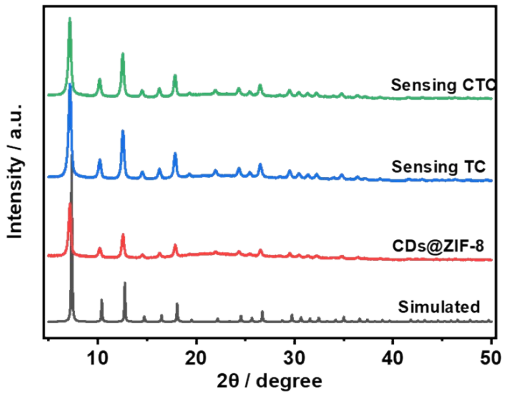

Fig. S23. PXRD of **CDs@ZIF-8** after being immersed in the solutions of TC and CTC.

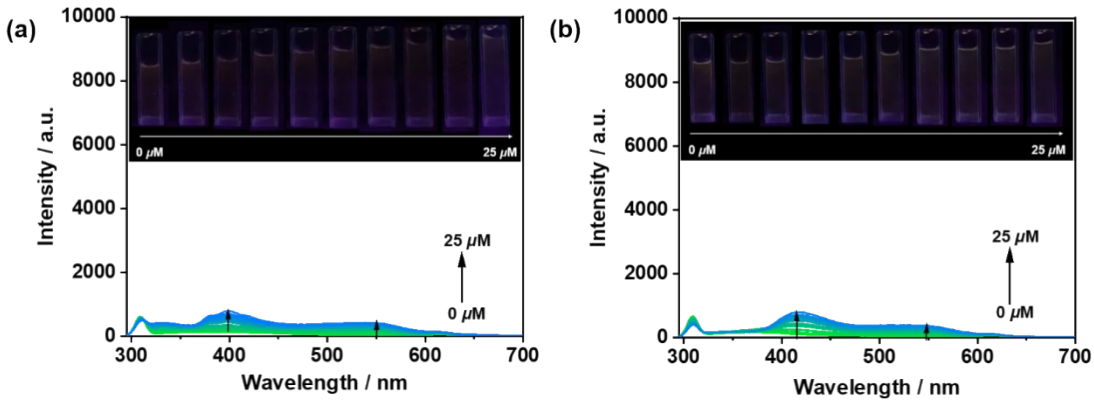

Fig. S24. (a) and (b) Fluorescence spectra of different concentrations of TC and CTC.

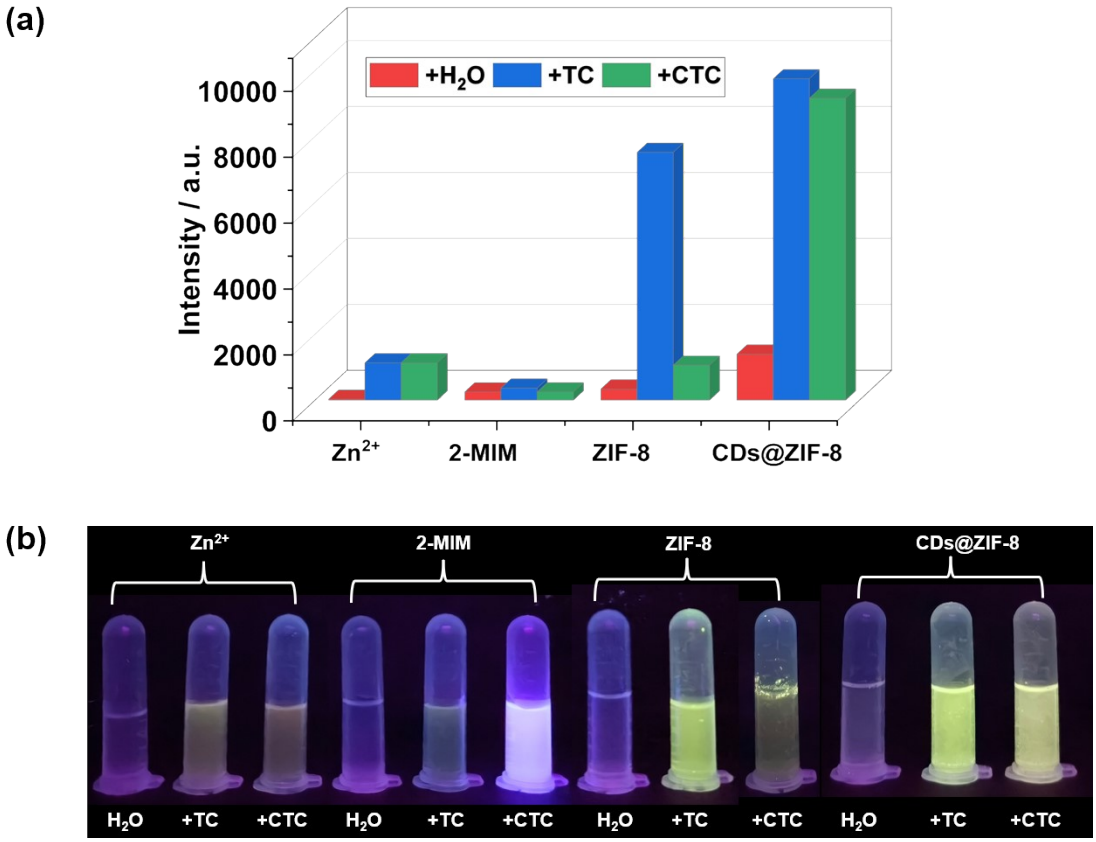

Fig. S25. (a) Statistical results of fluorescence intensity measured at 492 nm after dispersing Zn^{2+}, 2-MIM, **ZIF-8**, and **CDs@ZIF-8** in H_2O, TC, and CTC solutions, respectively; (b) Corresponding fluorescence images under 365 nm ultraviolet light irradiation.

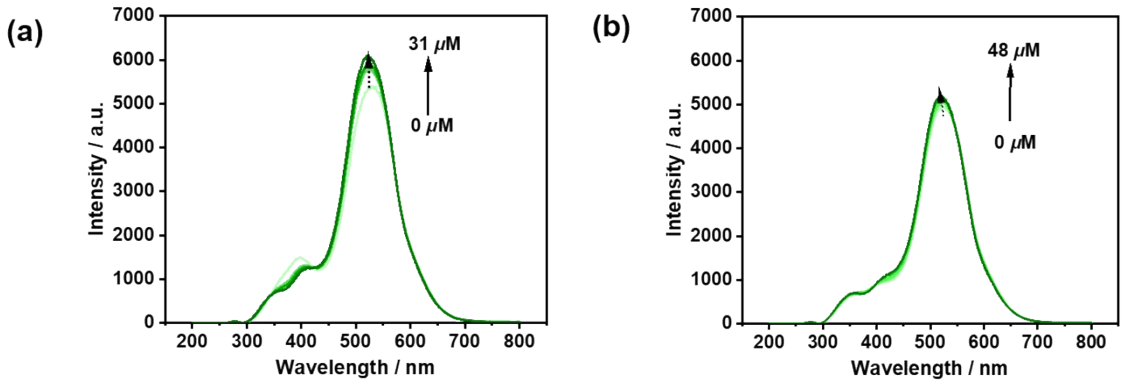

Fig. S26. (a) and (b) Fluorescence spectra of CDs with different concentrations of TC and CTC.

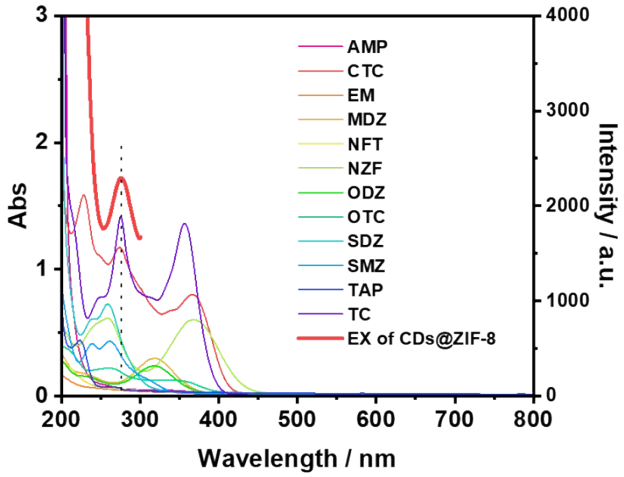

Fig. S27. UV−vis absorption spectra of various antibiotic solutions and excitation spectra of **CDs@ZIF-8.**

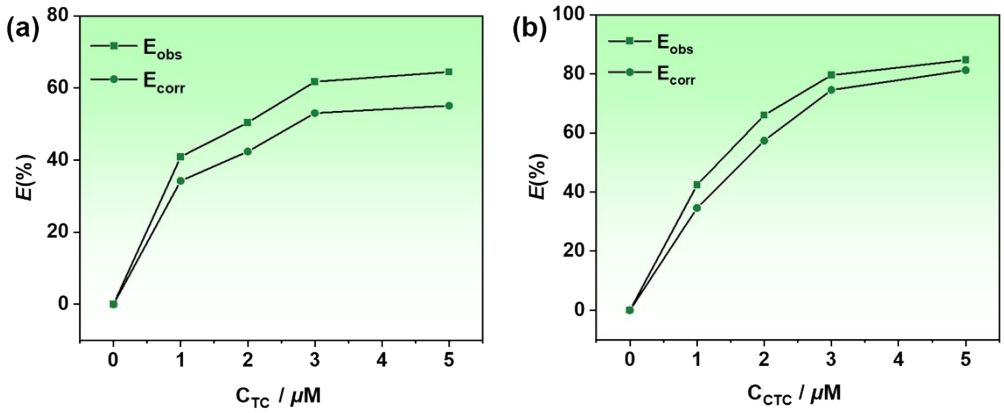

Fig. S28. (a) and (b) Variation trend of the inhibition efficiency with the concentration of TC and CTC under the influence of the IFE.

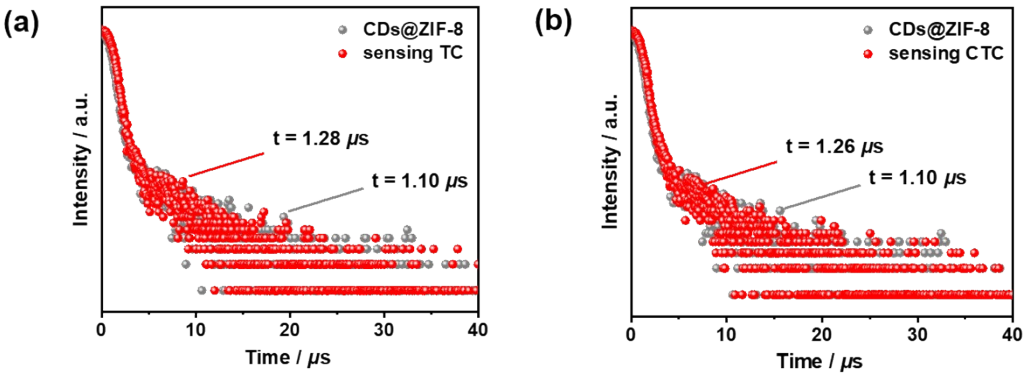

Fig. S29. (a) and (b) The luminescence lifetime decay curves of **CDs@ZIF-8** and **CDs@ZIF-8** with TC and CTC.

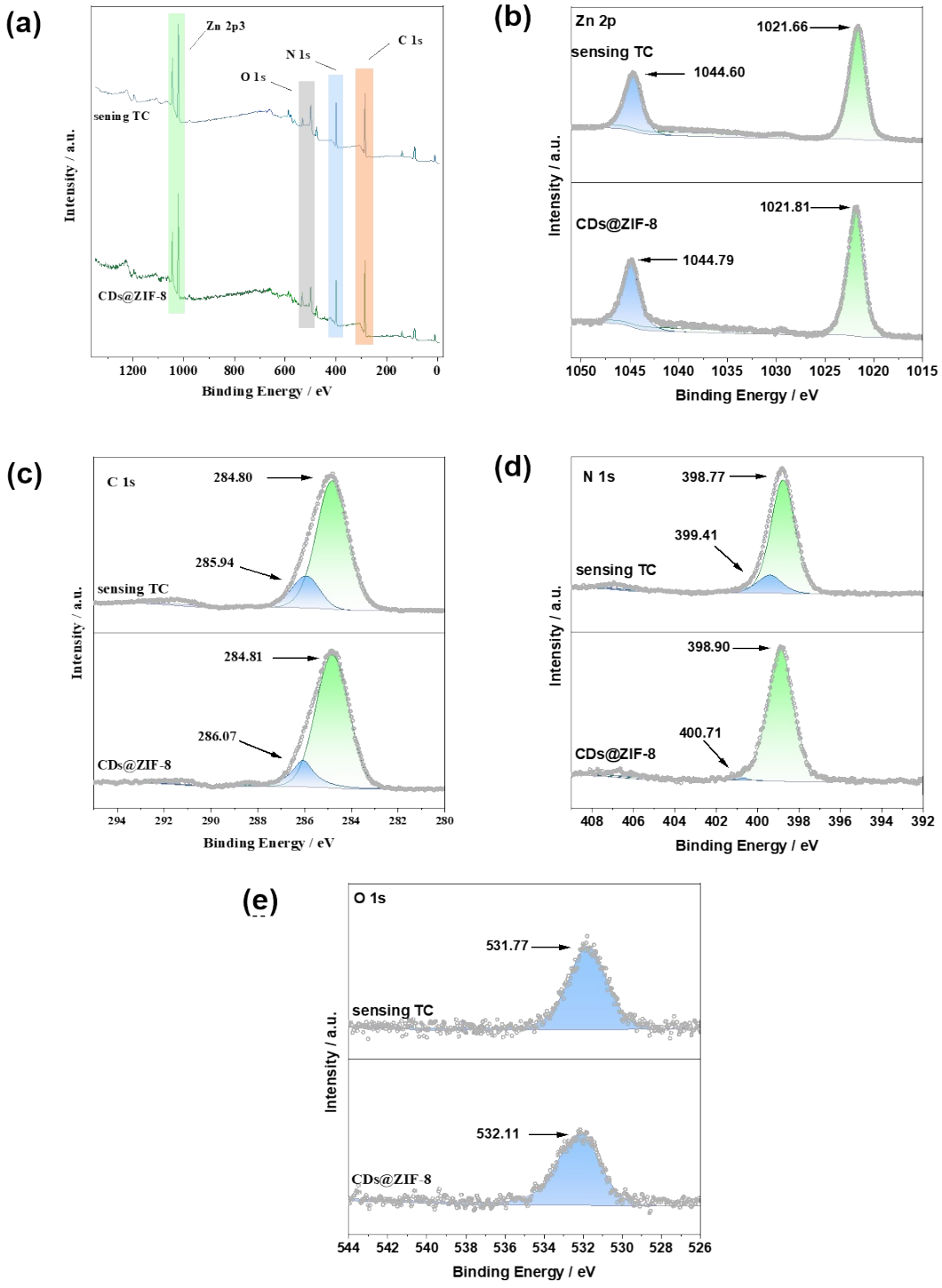

Fig. S30. (a-e) XPS spectra of **CDs@ZIF-8** before and after immersion in TC and high resolution regions of Zn2p, C1s, N1s and O1s, respectively.

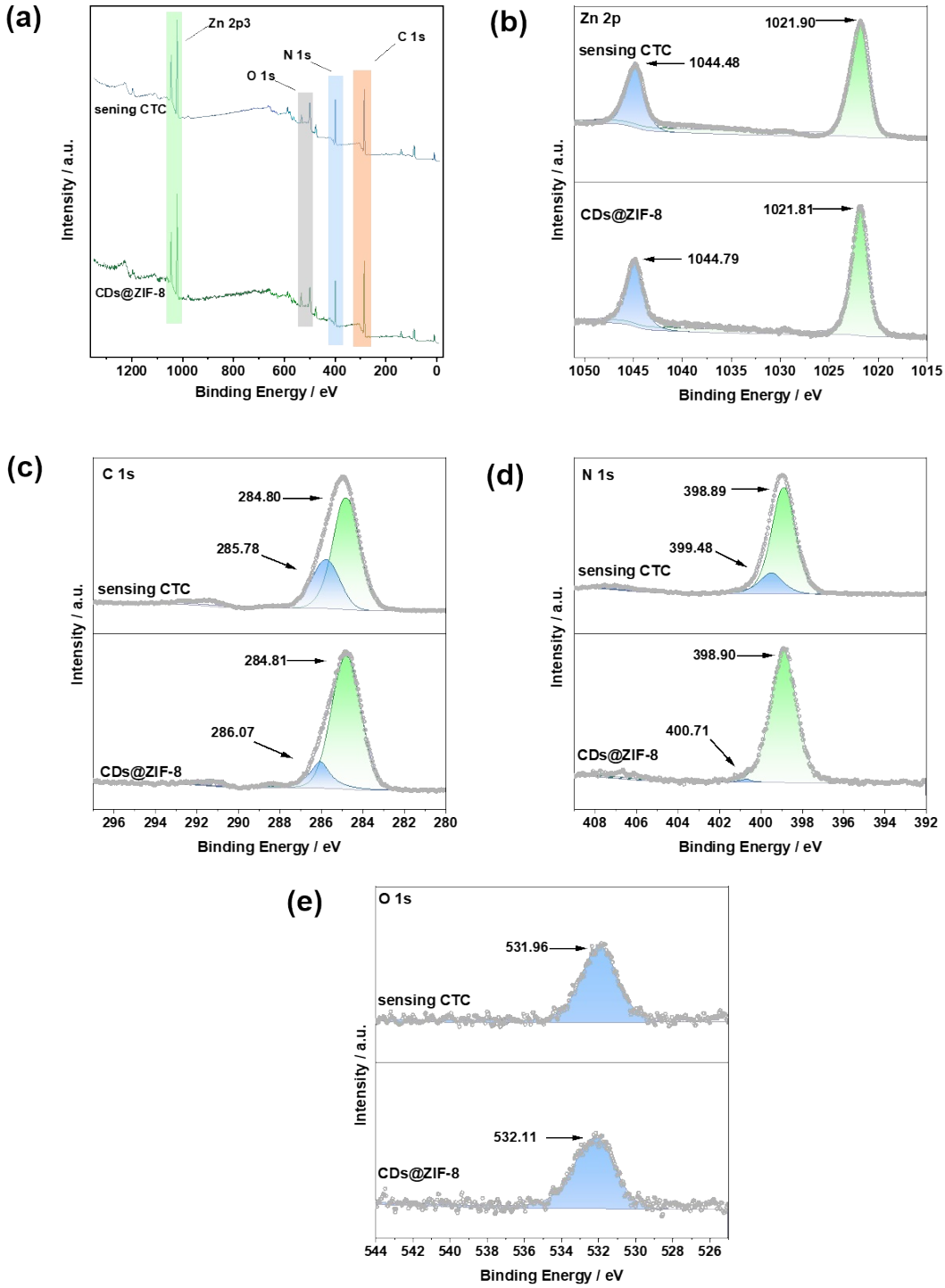

Fig. S31. (a-e) XPS spectra of **CDs@ZIF-8** before and after immersion in CTC and high resolution regions of Zn2p, C1s, N1s and O1s, respectively.